Gpr161 anchoring of PKA consolidates GPCR and cAMP signaling

Verena A. Bachmann[a,1], Johanna E. Mayrhofer[a,1], Ronit Ilouz[b], Philipp Tschaikner[c], Philipp Raffeiner[a], Ruth Röck[a], Mathieu Courcelles[d,e], Federico Apelt[f], Tsan-Wen Lu[b,g], George S. Baillie[h], Pierre Thibault[d,i], Pia Aanstad[c], Ulrich Stelzl[f,j], Susan S. Taylor[b,g,2], and Eduard Stefan[a,2]

[a]Institute of Biochemistry and Center for Molecular Biosciences, University of Innsbruck, 6020 Innsbruck, Austria; [b]Department of Chemistry and Biochemistry, University of California, San Diego, CA 92093; [c]Institute of Molecular Biology, University of Innsbruck, 6020 Innsbruck, Austria; [d]Institute for Research in Immunology and Cancer, Université de Montréal, Montreal, QC, Canada H3C 3J7; [e]Département de Biochimie, Université de Montréal, Montreal, QC, Canada H3C 3J7; [f]Otto-Warburg Laboratory, Max Planck Institute for Molecular Genetics, 14195 Berlin, Germany; [g]Department of Pharmacology, University of California, San Diego, CA 92093; [h]Institute of Cardiovascular and Medical Sciences, University of Glasgow, Glasgow, G12 8QQ, United Kingdom; [i]Department of Chemistry, Université de Montréal, Montreal, QC, Canada H3C 3J7; and [j]Institute of Pharmaceutical Sciences, Pharmaceutical Chemistry, University of Graz, 8010 Graz, Austria

Scaffolding proteins organize the information flow from activated G protein-coupled receptors (GPCRs) to intracellular effector cascades both spatially and temporally. By this means, signaling scaffolds, such as A-kinase anchoring proteins (AKAPs), compartmentalize kinase activity and ensure substrate selectivity. Using a phosphoproteomics approach we identified a physical and functional connection between protein kinase A (PKA) and Gpr161 (an orphan GPCR) signaling. We show that Gpr161 functions as a selective high-affinity AKAP for type I PKA regulatory subunits (RI). Using cell-based reporters to map protein–protein interactions, we discovered that RI binds directly and selectively to a hydrophobic protein–protein interaction interface in the cytoplasmic carboxyl-terminal tail of Gpr161. Furthermore, our data demonstrate that a binary complex between Gpr161 and RI promotes the compartmentalization of Gpr161 to the plasma membrane. Moreover, we show that Gpr161, functioning as an AKAP, recruits PKA RI to primary cilia in zebrafish embryos. We also show that Gpr161 is a target of PKA phosphorylation, and that mutation of the PKA phosphorylation site affects ciliary receptor localization. Thus, we propose that Gpr161 is itself an AKAP and that the cAMP-sensing Gpr161:PKA complex acts as cilium-compartmentalized signalosome, a concept that now needs to be considered in the analyzing, interpreting, and pharmaceutical targeting of PKA-associated functions.

interaction network | molecular interactions | scaffolding function | phosphorylation | primary cilium

Scaffolding proteins act as flexible organizing centers to consolidate and propagate the cellular information flow from activated cell-surface receptors to intracellular effector cascades. Activated G protein-coupled receptors (GPCRs) engage pleiotropic scaffolds to recruit cytoplasmic downstream effector molecules (1–4). Thus, compartmentalized GTPases, kinases, and phosphatases act as GPCR-linked molecular switches to spatially and temporally control signal propagation. In the classic view of GPCR signaling, extracellular ligands bind to the receptor, which catalyzes the intracellular GDP/GTP exchange and activation of receptor-associated trimeric G protein (α:β:γ) combinations. GPCR signaling and trafficking involve G protein-dependent and -independent intracellular interactions with scaffolds, such as β-arrestin and A-kinase anchoring proteins (AKAPs) (1, 2, 5, 6). Receptor-interacting proteins and kinase activities contribute to the fine-tuning of GPCR localization and activities (4, 7–9). Different AKAPs coordinate and compartmentalize diffusible second-messenger responses through anchoring of cAMP-dependent type I or type II protein kinase A (PKA) holoenzymes, composed of a regulatory subunit (R) dimer and two catalytic (PKAc) subunits, to discrete subcellular localizations (1, 10, 11). The four R subunits (RIα/β or RIIα/β) have different expression patterns and are functionally nonredundant. The growing family of AKAPs are functionally diverse; however, all AKAPs contain an amphipathic helix, which

accounts for nanomolar binding affinities to PKA R subunit dimers (12, 13). Moreover, additional components of the cAMP signaling machinery, such as GPCRs, adenylyl cyclases, and phosphodiesterases, physically interact with AKAPs (1, 5, 11, 14). Mutations activating cAMP/PKA signaling have been shown to contribute to carcinogenesis or degenerative diseases, and inactivating mutations have been linked to hormone resistance (15–20). In-depth analyses of transient protein–protein interactions (PPIs) of PKA, along with the phosphorylation dynamics, have the potential to reveal conditional signal flow and thus may help to explain pathological implications of cAMP/PKA signaling. Such a strategy will lead to a better understanding of cAMP-signaling, which boosts proliferation in many cell types but inhibits cell growth in others (21, 22). Using a proteomics approach, we discovered that an AKAP motif is embedded within the C-terminal tail of Gpr161, an orphan GPCR that is associated with the primary cilia (23). We confirmed the direct functional interaction of Gpr161 with PKA and showed that it has absolute specificity for RI subunits. We show that Gpr161 is not only a RI-specific AKAP but also a PKA substrate. Finally, in

Significance

At the plasma membrane an array of more than 800 G protein-coupled receptors (GPCRs) receive, convert, amplify, and transmit incoming signals. Activated GPCRs team-up with intracellular scaffolding proteins to compartmentalize signal transmission. Scaffolds, such as β-arrestin and A-kinase anchoring proteins (AKAPs), function as a physical nexus between receptors and molecular switches. Typically, these receptor-bound AKAPs recruit protein kinase A (PKA) to assemble dedicated polyvalent signaling complexes that are spatially and temporally confined. Here, we report that the orphan GPCR, Gpr161, is a PKA substrate and also has an AKAP motif embedded in its C-terminal tail. Our results suggest that Gpr161, by directly recruiting type I PKA holoenzymes to the receptor, creates a cAMP-sensing signalosome. Furthermore, we propose that Gpr161 plays a role in recruiting isoform-specific PKA complexes to primary cilia.

experiments with zebrafish embryos we demonstrate that Gpr161 receptors recruit RI to primary cilia.

Results

Identification of a Binary PKA and Gpr161 Interaction. PPI information is typically generated in exogenous systems, such as yeast two-hybrid approaches, or from affinity purification followed by mass spectrometry of overexpressed and tagged proteins (24, 25). Here, we affinity-purified endogenous PKA complexes from the osteosarcoma cell line U2OS using PKA-selective Rp-8-AHA-cAMP-agarose resin after selective activation of β-2 adrenergic receptors (β₂AR) (9), and within this set we identified several novel PPIs. Following phosphoproteomic analyses (liquid chromatography–mass spectrometry, LC-MS), we generated an integrated PKA PPI network representing a consistent set of PKA-associated proteins. We confirmed the enrichment of all four PKA R subunits and two PKA catalytic subunits (PKAcα/β). We organized the interaction partners in a fan-shaped pattern surrounding the centered PKA subunits, providing a combined overview of 92 Rp-8-AHA-cAMP affinity-purified proteins that were significantly enriched compared with the control experiment (excess of cAMP) (Figs. S1 and S2 and Dataset S1). We mapped all of the detected phosphorylation sites and present copurified phosphoproteins with their identified sites in a PKA-centric illustration, including all 76 known phosphorylation sites and 33 potential PKA-specific phosphorylation sites (Fig. 1*A*). With the Rp-8-AHA-cAMP–bound PKA subunits, we enriched numerous AKAPs, which are known binary interaction partners of R subunits. This approach revealed macromolecular PKA complexes that contain additional proteins involved in functions, such as protein transport, RNA binding, and discrete posttranslational modifications. Our analyses also identified a large set of proteins attributed to metabolic signaling, thus both underlining established and revealing novel connections of PKA to metabolic pathways. Interestingly, not easily accessible interactors, like membrane receptors and channels, were also identified in the macromolecular PKA complexes. Of these, the orphan GPCR, GPR161, is of particular interest. In mouse, Gpr161 was recently shown to antagonize Hedgehog (Hh) signaling at the primary cilium (23). Gpr161 acts as a Gαs-coupled receptor and activates PKA, a central negative regulator of Hh signaling (Fig. 1*B*) (23). The identification of Gpr161 in the macromolecular PKA complex, together with the phosphorylation of a canonical PKA phosphorylation consensus site in the cytoplasmic C-terminal tail of Gpr161, raises the question of how possible physical interactions between PKA and Gpr161 might contribute to regulation of Gpr161 function. Interestingly, the Gpr161 C terminus (CT)

was shown previously to be critical for the function of Gpr161 (Fig. 1*B*) (26).

To facilitate the functional analyses of the cytoplasmic tail of murine Gpr161, we first generated different glutathione-Sepharose-transferase (GST) expression constructs to more rigorously investigate complex formation with PKA. In GST pulldown assays we precipitated endogenous PKA subunits from cell lysates with GST- $CT^{340-528}$ and found a significant enrichment of endogenous RI:PKAc complexes. No binding of RIIβ was detectable. Addition of an excess of cAMP to the precipitation reaction promoted PKA dissociation. Whereas increased cAMP levels diminished PKAc binding to RI, the GST-$CT^{340-528}$:RI complex was insensitive to cAMP-binding (Fig. 1*C*). These data indicate that binding of PKAc to Gpr161 is mediated through RI subunits. To identify the specific amino acid residues of Gpr161 that are responsible for RIα binding, we used a peptide array assay. Overlapping 25-mer peptides derived from the human Gpr161-*CT* sequence were spotted onto a membrane and overlaid with recombinant RIα-*his*⁶, as previously described (27, 28). In the Gpr161-CT we identified only one possible binding site for RIα. Next, the helix propensity of the receptor CT was determined predicting a helical content of the peptide spanning approximately from D459/S460 to N476 that is flanked by L458 at the N terminus and by L477 at the C terminus (Fig. 1*D* and Fig. S3). This region corresponded to the peptides that were identified in the peptide array.

To perturb the integrity of the predicted helix structure, the highlighted L465 was substituted with proline. *His*⁶-tagged bacterial expression constructs of the Gpr161-$CT^{378-528}$ were generated. In affinity purifications using Ni-NTA resin, we copurified significant amounts of untagged RIα with $CT^{378-528}$ but observed no PPI with the $CT^{378-528}$[L465P] mutant of Gpr161 (Fig. 1*E*). A subsequent cAMP-precipitation showed the stability and specificity of this binary PPI in vitro (Fig. S4). The selective in vitro enrichment of RIα with $CT^{378-528}$ supports the hypothesis that the CT of Gpr161 interacts directly with recombinant RIα.

Functional Characterization of the AKAP Motif in Gpr161. The common PPI motif found in all AKAPs is an amphipathic helix (1, 11, 13). The helical wheel projection shown in Fig. 2*A* points to the existence of an amphipathic helix in the CT of Gpr161, spanning from the N-terminal L458 to the C-terminal L477. To ease the assignment of the amino acids that might contribute to PPI, we have chosen the "helix numbering" 1–20 (corresponds to Gpr161⁴⁵⁸⁻⁴⁷⁷). The evolutionary conserved amino acids are highlighted in red (Fig. 2 *A*, *D*, *E*). With different recombinant GST-CT variants of Gpr161 we repeated the pulldown experiments
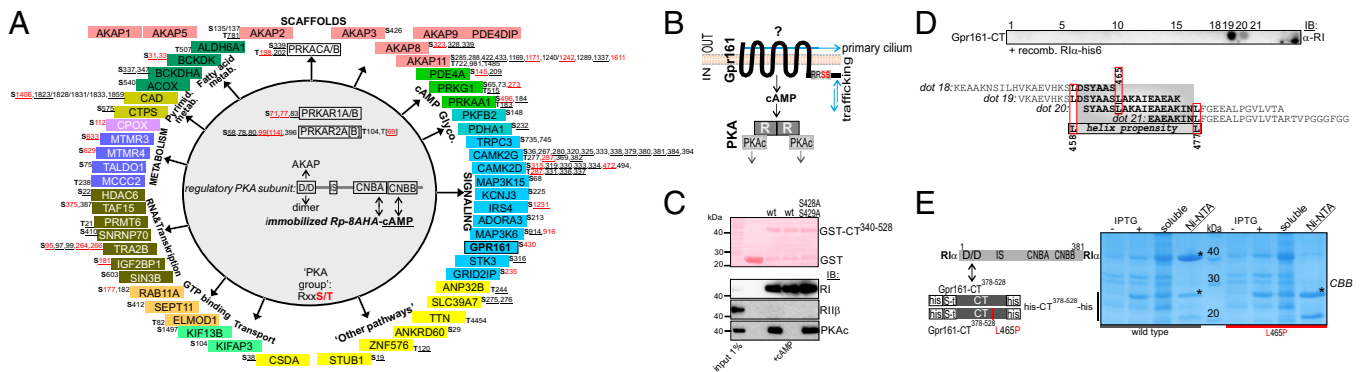

Fig. 1. PKA phosphoprotein interactome and Gpr161:RI interaction. (*A*) Phosphoproteins of affinity-purified PKA complexes are listed. Underlining marks previously described p-sites; red labeling highlights PKA group sites with a phosphorylated RxxS/T sequence motif. (*B*) Schematic illustration of Gpr161 trafficking and PKA signaling; cAMP binds R subunits and activates PKAc. (*C*) GST pulldown experiments of endogenous PKA subunits from HEK293 cell lysates in the presence or absence of 5 mM cAMP using GST and GST-CT (murine Gpr161-Carboxy-terminus³⁴⁰⁻⁵²⁸) hybrid proteins. (*D*) Spotted peptides (25-mers, 15-aa overlap) of human Gpr161-CT were overlaid with recombinant RI. Immunoblotting (IB) has been performed with a monoclonal anti-RI antibody. The helix propensity of this part of Gpr161-CT (flanked by L458 and L477) is shown. Indication of L465. (*E*) Following bacterial coexpression of his⁶-tagged $CT^{378-528}$ (wild-type and L465P) and untagged RIα we purified complexes using Ni-NTA resin. Representative experiment from n = 3. Asterisks (*) indicate specific Coomassie brilliant blue-stained bands.

BIOCHEMISTRY

with recombinant RIα-his[6] in vitro. All truncated hybrid variants containing the predicted helix showed binary interaction with RIα. Once again the complex formation in the affinity purifications was insensitive to cAMP binding to RIα. The GST-$CT^{340–528}$ mutant containing the L465P (corresponds to L8 helix numbering) substitution showed no binding to RIα (Fig. 2B). These experiments confirmed a binary PPI between the CT of Gpr161 and RIα in vitro and localized the interaction site to Gpr161$^{458–477}$. Moreover, our results strongly support the prediction that a canonical amphipathic helix in the GPCR-CT mediates PPI with PKA RI subunits, as has been described in detail for all other members of the AKAP family. In experiments with cell lysates we observed a similar pattern of PPI with RI. Endogenous RIIβ did not bind to any of the GST-fused CTs (Fig. S5A). With overexpressed Gpr161 variants we repeated cAMP-precipitation experiments as performed for Fig. 1A and Figs. S1 and S2, showing that cAMP-bound R subunits are sufficient for the precipitation of full-length Gpr161-Venus-YFP. In comparison, the Gpr161-ΔCT (=deletion of the CT) mutant showed no PPI (Fig. S5B). These data confirm our peptide array results and demonstrate that the CT of Gpr161 mediates binary PPI with the RI PKA subunit. Next, we subjected a 25-mer peptide of the Gpr161-CT$^{457–481}$ to fluorescence polarization measurements with full-length RIα and RIIβ. We observed selective and high-affinity binding of the peptide to RIα with a K_d of 6.0 nM ($\pm$0.1); in contrast, no binding to the RIIβ homodimer was observed (Fig. 2C). This finding is in agreement with the pulldown assays illustrated in Fig. 1C and Fig. S5A, which show exclusive RI binding to the different CT variants.

In dot blot analyses we compared binding of recombinant RIα to different amphipathic helices of selected AKAPs (29). In this in vitro assay, specific binding of RIα to sequences consisting of distinct parts of the predicted amphipathic helix in Gpr161-CT was confirmed; binding was abolished with peptides containing Pro substitutions located in the specific R binding pockets of AKAPs (Fig. S6). In structure-based alignments of Gpr161 with RI-specific AKAPs and dual-specific AKAPs, we identified semiconserved residues that bind into the hydrophobic groove of the RIα-dimer and docking (D/D) domain (shown in gray in Fig. 2D). In addition, we observed partial conservation of the flanking Leu residues, L458 and L477, respectively. Based on these observations, we generated a structure model consisting of the RIα-D/D domain in complex with the Gpr161 peptide 456–478. Again, to ease the assignment of the relevant amino acids, they are numbered from 1 to 20 (corresponding

to Gpr161$^{458–477}$, helix numbering) with the conserved amino acids that might contribute to PPI highlighted in red in Fig. 2D.

The presented structure model is based on the previously published complex of the RIα-D/D domain, with the D-AKAP2 peptide (30). The RIα-D/D structure consists of an antiparallel, four-helix bundle that forms the interaction surface. The Gpr161 peptide seems to dock via the six conserved binding pockets (shown in red in Fig. 2E) onto the hydrophobic groove of the RIα dimer. Interestingly, E13 (corresponding to Gpr161 E470) in the Gpr161 peptide is part of the hydrophilic helix and an outlier in the assignment of binding pockets with other amphipathic helices (Fig. 2 D and E). The structure model shows that the E side-chain points to the linker between the two RI helices. We assume that the negative charge of E13 can be compensated by the neighboring residue in RIα K17. The structure comparison of the D/D domains of RIα with RIIα indicate a more extended hydrophobic surface at the N terminus of RIα that includes a third helix (α0-Helix) instead of a short strand that is a conserved feature of the RII subunits. The assessment of the AKAP sequences, available RIα and RIIα structures, and the presented structural model provide a possible explanation for the selective RI-binding to Gpr161-CT (13, 30). In the sequence alignment presented in Fig. 2D we highlight that, in addition to the four hydrophobic pockets, the N- and C-terminal Leu residues (L1, L20) in RI create two additional pockets, which might account for the selective binding of Gpr161 to RI. We tested this hypothesis in experiments using a cell-based PPI reporter.

Quantification of Cellular Gpr161 and RIα/β Complexes. The *Renilla* luciferase (*R*luc)-based protein-fragment complementation assay (PCA) was applied to characterize Gpr161:RI interactions directly in living cells (31, 32). The *R*luc PCA PPI reporter was used to characterize the binding interface and the involvement of PKA phosphorylation (Fig. 3A). First we confirmed RIα homodimer formation and we demonstrated specific binding of RIα to Gpr161 in HEK293 cells. With the Gpr161[L465P] mutant the PPI signal decreased significantly. In the control experiments, no specific signals for PPIs between the *R*luc PCA-tagged Gpr161-F[2] with F[1]-F[1] or PKI-F[1] were observed (Fig. 3B). Second, we tested the involvement of Ser428 and Ser429 [PKA phosphorylation consensus site (RRSS)] on complex formation of Gpr161:RIα. In *R*luc PCA analyses, we observed that none of the S428 or S429 amino acid substitutions with either Ala or Asp had a major
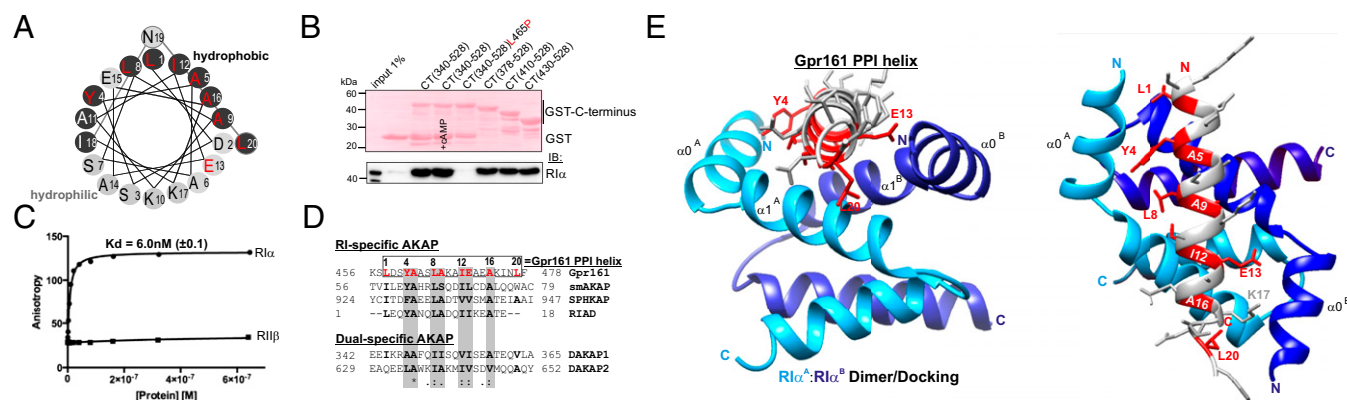

Fig. 2. Interaction of Gpr161:RIα in vitro and in silico. (A) Helical wheel projection of the helix propensity of Gpr161-CT from L458 to L477 (murine Gpr161 numbering; helix numbering 1–20). Red labeling indicates conserved amino acids potentially involved in PPI with RI. (B) GST pulldown experiments of recombinant RIα in the presence or absence of 5 mM cAMP using indicated GST-CT fusions of Gpr161 including the $CT^{340–528}$-L465P mutant. (C) Binding analyzes of full-length RIα (●) or full-length RIIβ (■) to the 5-carboxyfluorescein (5-FAM)–labeled peptide of Gpr161 (amino acids 457–481; 25-mer) by steady-state fluorescence anisotropy measurements. $\pm$SD from $n = 3$ independent experiments. (D) Structure-based alignment of Gpr161 (murine) with RI-specific and dual-specific AKAPs (human). The four binding pockets are highlighted in gray. Conserved and possibly PPI-involved amino acids are shown in bold. Gpr161 residues that seem to participate in the interaction with the hydrophobic groove of the RI-D/D domain are highlighted in red. Identity (*) and similarities (: and .) are indicated. (E) Structural model of RIα D/D domain in complex with Gpr161-CT$^{456–478}$ peptide. Crystal structure of RIα D/D-domain:DAKAP-2 peptide (PDB ID code 3IM4) was used to build the model. The DAKAP-2 sequence was substituted with the predicted amphipathic helix sequence of Gpr161-CT$^{456–478}$. Side and top view of the model are shown. The monomers of the RIα D/D domain are depicted in blue and the Gpr161 helix is shown gray with PPI-relevant amino acids highlighted in red (helix numbering 1–20).

impact on the RIα:Gpr161 PPI. Third, the involvement of the N- and C-terminal Leu (L458 and L477; Fig. 3C) on complex formation was tested. Substitution of both Leu with Ala reduced the complex formation of Gpr161 with RIα, thus confirming that the helix flanking Leu also contribute to the R subunit-specific PPI of RI and Gpr161. The specific importance of the flanking regions for RI binding (Fig. 3C) was highlighted in the recent structure of the smAKAP (PKA RIα-specific AKAP) with the RIα dimerization domain (33). Similar to Gpr161, smAKAP has affinity for RI in the low nanomolar range (7 nM). However, in contrast to Gpr161, smAKAP has affinity for RII as well (53 nM). In the smAKAP two flanking residues, an N-terminal Ile and a C-terminal Trp, form two additional hydrophobic pockets, creating a hydrophobic interface with six interaction pockets in total. Gpr161 and smAKAP are the only two AKAPs so far that have single nanomolar affinity for RI subunits.

Through the N-terminal D/D domain, R subunits dimerize and interact with the amphipathic helices of AKAPs (11, 34). Therefore, a perturbation of the integrity of the D/D domain would specifically affect AKAP interaction. Recently, the patient mutation RIβ[L50R], localized in the D/D region of RIβ, has been associated with a neurodegenerative disorder causing accumulations of RIβ in neuronal inclusions (20). The L50R mutation in the core of the antiparallel four-helix bundle in RIβ has been discussed to affect RIβ dimerization (20). We showed that in addition to RIα, RIβ also specifically binds to Gpr161. Dimer formation of R subunits is the precondition for AKAP binding. In the Rluc PCA measurements, we observed a substantial reduction of RIβ[L50R]:Gpr161 complexes (Fig. 3D). These results further support the idea that Gpr161 contains intrinsic AKAP properties by binding to dimeric RIβ-D/D.

Subcellular Localization of Gpr161 and PKA Subunits. To investigate the functional importance of the PKA:Gpr161 interaction, we determined the subcellular localization of the Venus-YFP tagged Gpr161 in HEK293 cells. The wild-type receptor was mainly localized to cytoplasmic compartments. Consistent with a previous report (26), the receptor lacking the last 155-aa residues (Gpr161-ΔCT) was primarily localized to the plasma membrane (Fig. S7A). We used the same constructs for coprecipitation studies. Whereas immunoprecipitation (IP) of wild-type Gpr161 copurified PKA complexes, IP using the Gpr161-ΔCT variant showed no PPI with PKA subunits (Fig. S7B). These results

suggest that the Gpr161-CT is relevant for both plasma membrane targeting and RI interaction. For colocalization studies we used an mCherry-tagged receptor and RIα-GFP constructs. Following transient overexpression of the Gpr161-mCherry variants in single transfection studies, we confirmed cytoplasmic accumulation of the wild-type receptor. The L465P and the phosphorylation-deficient S428A/S429A mutants all showed a similar localization. In the single transfections, RIα-GFP was found throughout the cytoplasm showing a speckled/punctate localization (Fig. 3E). Interestingly, upon coexpression of the wild-type and the S428A/S429A receptor mutant with RIα, a significant proportion of the Gpr161:RIα complex was recruited to the plasma membrane. Strikingly, with the Gpr161-L465P mutant we detected neither colocalization nor membrane recruitment (Fig. 3F). These data suggest an unexpected role for RI subunit binding in plasma membrane targeting of Gpr161.

In the initial phosphoproteomic screen, we found that Gpr161 is phosphorylated at the PKA consensus site position RRSS429 (corresponding to human Gpr161 S430) (Fig. 1A). Following transient transfections of HEK293 cells stably expressing β_2AR, the phosphorylation patterns of Venus-YFP tagged wild-type receptors, as well as the S428A/S429A and L465P mutants, were analyzed. We elevated cellular cAMP-levels with Forskolin or the βAR agonist isoproterenol. Following IP of Gpr161 variants, we tracked changes of their phosphorylation status with a PKA substrate antibody. In contrast to the L465P mutant, we found that the overexpressed wild-type receptor and S428A/S429A receptor mutant bound endogenous RI. Upon cAMP-elevation, we observed a significant increase in Gpr161 phosphorylation. With the Gpr161-S428A/S429A receptor mutant, however, we detected no phosphorylation signal at all, suggesting that S428/S429 is the primary target site for PKA phosphorylation. Moreover, the L465P receptor mutant, which does not compartmentalize PKA complexes, showed a significant reduction of Gpr161 phosphorylation following cAMP-elevation (Fig. 4A). These data indicate that Gpr161-compartmentalized type I PKA activity directly senses and integrates cAMP oscillations that in turn affect receptor phosphorylation.

Phosphorylation and Ciliary Localization of PKA Subunits and Gpr161. In mouse, Gpr161 has been shown to act as an antagonist of Hh signaling by promoting cAMP levels and activating PKA (23). Regulation of Hh signaling takes place in the primary cilium, and
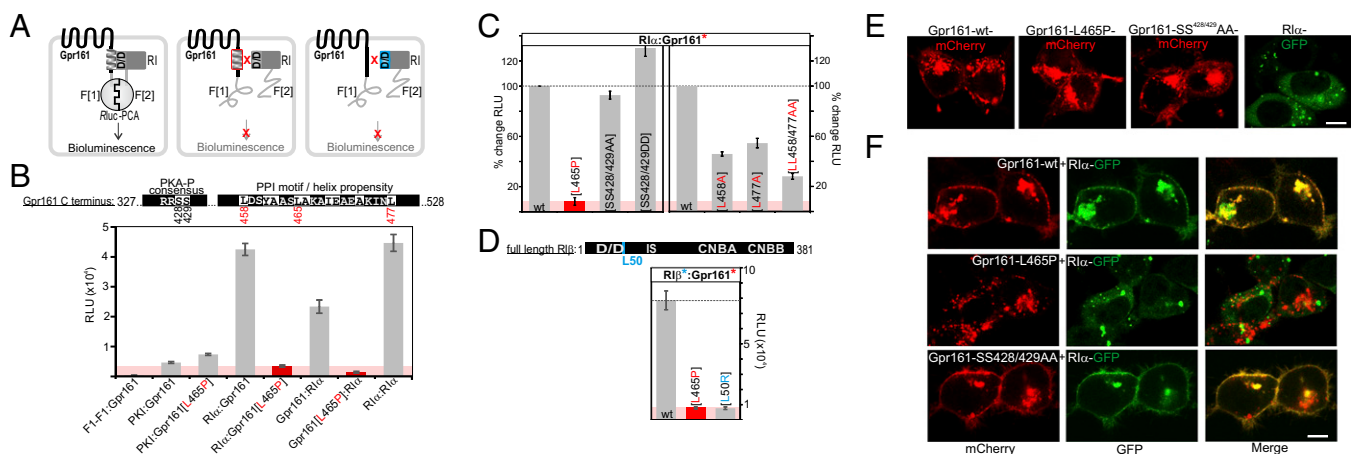
BIOCHEMISTRY

Fig. 3. Cellular PPIs and localization of Gpr161 variants. (A) Schematic illustration of the Rluc-PCA biosensor strategy to quantify PPIs of wild-type and mutated Gpr161 and RI in vivo. Mutated domains are highlighted in red/blue. (B) Shown are conserved sequence elements in the Gpr161-CT. Impact of L465P mutation of Gpr161-F[1]/[2] on complex formation with RIα-F[1]/[2] (±SEM; representative of n = 3 independent experiments; murine Gpr161^{1–528}; NP_001297359.1). (C) Impact of Gpr161 mutations of the flanking Leu of the PPI-motif and the PKA phosphorylation consensus site on RIα:Gpr161 PPI. Read out: Rluc PCA (±SEM of at least n = 4 independent experiments). (D) Impact of the L50R mutation on RIβ:Gpr161 PPI; Rluc PCA measurements (±SEM; representative of n = 3). (E) Subcellular localization of mCherry-tagged Gpr161 or GFP-tagged RIα hybrid proteins in HEK293 cells. (Scale bar, 5 μm.) (F) Subcellular localization of coexpressed mCherry-tagged Gpr161 variants and GFP-tagged RIα in HEK293 cells. (Scale bar, 5 μm.)

Gpr161, like Hh pathway components, localizes to the cilium (23, 35–38). Although the mechanisms controlling PKA activation in Hh signaling have long remained elusive, a recent study of the ciliary proteome showed that RIα, which has previously been implicated in Hh signaling (39), localizes to the ciliary shaft (40). Sequence comparisons showed that both the AKAP motif and the PKA phosphorylation sites are conserved in the zebrafish Gpr161 (Fig. 4B). To test the hypothesis that Gpr161 may act as an AKAP to localize RIα to the primary cilium, we injected zebrafish embryos with Gpr161-mCherry and RIα-GFP mRNAs. The zebrafish experimental protocols were approved by the Austrian Ministry for Science and Research (GZ BMWF-66.008/ 0019-II/3b/2013). First, we confirmed that wild-type Gpr161 localizes to the primary cilium also in zebrafish (Fig. 4C). The ciliary localization of Gpr161 was significantly not affected by the PKA phosphorylation-deficient mutations S428A/S429A (Fig. 4C). However, we observed that the introduction of negative charges at the positions S428D/S429D (phosphomimetic) significantly reduced the percentage of Gpr161-mCherry-positive cilia (Fig. 4C). Coexpression of Gpr161-mCherry and RIα-GFP revealed that the majority of wild-type Gpr161-mCherry-positive cilia were also positive for RIα-GFP (Fig. 4D). This ciliary localization of RIα-GFP was significantly reduced upon introduction of the L465P mutation, further confirming that Gpr161 recruits PKA type I holoenzymes to the primary cilium (Fig. 4D). These results collectively support the idea that Gpr161 is itself an AKAP that directly recruits PKA complexes to the primary cilium.

Discussion

The idea that scaffolding proteins act as organizing centers to converge and redirect the information flow has evolved over the last two decades (3, 6). Diverse scaffolds assemble, spatially and temporally, flexible signaling nodes consisting of various signaling proteins, such as GTPases, kinases, and phosphatases. In the classic view, scaffolds like AKAPs, β-arrestin, Ksr1, and postsynaptic-density proteins act as connectors between receptors and downstream effectors (1, 2, 3, 41). Here, we show that Gpr161 itself contains a high-affinity AKAP binding motif that is specific for type I PKA holoenzymes. Several examples showing how AKAPs recruit type II PKA to distinct membrane receptors have been described (11, 42, 43). Gpr161, however, appears to act differently, in that it binds PKA directly. This finding has implications for our understanding of how kinase anchoring and

receptor-mediated compartmentalization of PKA contribute to receptor and kinase functions. Based on biochemical and cell biological interaction data, along with in silico modeling of the interface, we propose a selective and high-affinity interaction of Gpr161 with PKA RI-subunits. We show evidence for an extended classic PPI motif in the cytoplasmic C-terminal tail of Gpr161, and demonstrate that this motif functions as a potential amphipathic helix for RI subunit interaction. This finding would be consistent with other AKAPs, which contain amphipathic helices acting as PPI interfaces for either RI or RII subunits. Using a cell-based reporter for binary PPIs, we demonstrate that the flanking Leu of the PPI motif represent additional hydrophobic interaction sites, which may account for the highly RI-specific interaction (Fig. 2). Consistent with the idea that AKAPs act to recruit PKA to its substrates, we show that Gpr161-dependent recruitment of endogenous type I PKA complexes is required for efficient Gpr161 phosphorylation (Fig. 4A). Prevention of Gpr161: RI complex formation significantly reduced cAMP-induced Gpr161 phosphorylation (Fig. 4A). We propose that, in a physiological setting, complex formation is required for integrating compartmentalized cAMP fluxes. In HEK293 cells, we observed that overexpression of both Gpr161-mCherry and RIα-GFP resulted in a change of the localization of both proteins. Binary complex formation of RI mediated through the CT of Gpr161 promotes the localization of the receptor to the plasma membrane by a mechanism that remains to be resolved (Fig. 3F). Interestingly, a Gpr161 construct missing the CT shows a similar PKA-independent plasma membrane localization (Fig. S7A), which results in functional consequences on Gpr161 signaling, as previously described (26). A recent study showed that activation of Hh signaling promotes Grk2- and β-arrestin–dependent export of Gpr161 from the primary cilium (37). Our results suggest that phosphorylation of Gpr161 by PKA also affects the ciliary localization of Gpr161, although how this might interact with Grk2/β-arrestins is unknown.

Although PKA acts as a major negative regulator in the Hh pathway, the mechanisms by which activation of Hh leads to the inhibition of PKA activity are not fully understood. Gpr161 has previously been shown to localize to the primary cilium and to antagonize Hh signaling by activating PKA in the absence of Hh ligands (44). Although Hh pathway components localize to the primary cilium, Hh-dependent regulation of PKA activity was proposed to take place at the basal body, based on the localization of the PKA RII subunit (45). However, a recent proteomics study
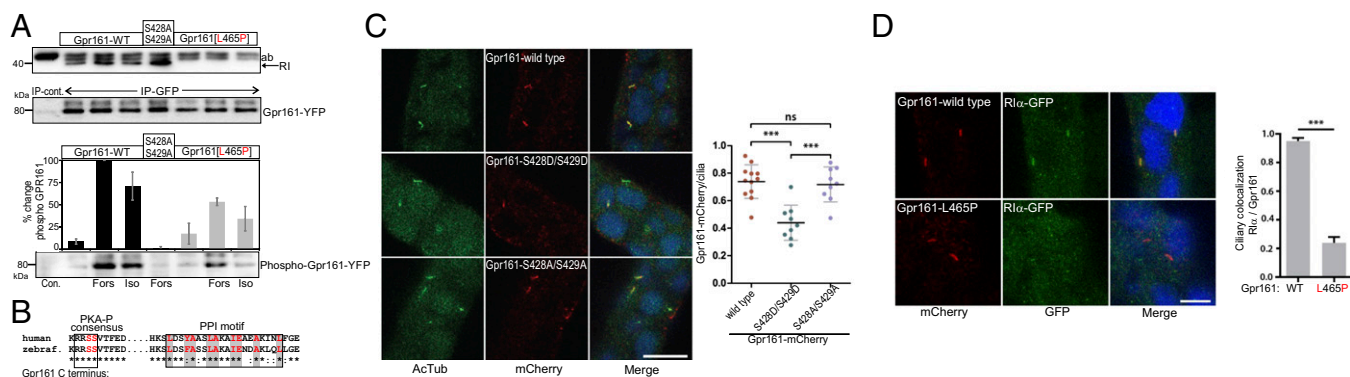

Fig. 4. Phosphorylation and ciliary localization of Gpr161:RIα complexes. (A) IP of Venus-YFP–tagged Gpr161 variants expressed in HEK293 cells following treatments with Forskolin (20 μM, 10 min) and isoproterenol (1 μM, 10 min). Densitometric quantification of $n = 4$ independent experiments, ±SEM; phospho-(K/R)(K/R)X(S*/T*) specific antibody. The IB with the RI antibody is taken from a different experiment (better separation of antibody and RI). (B) Sequence comparison of AKAP and phosphorylation motifs from human and zebrafish Gpr161-CT. (C) Subcellular localization of indicated Gpr161-mCherry variants and acetylated-Tubulin in zebrafish. (Scale bar, 10 μm.) The graph shows the ratio of Gpr161-positive cilia and the total number of cilia in a minimum of three sections from three independent experiments. P values were calculated using one-way ANOVA and Tukey's multiple-comparison post hoc test (***$P < 0.001$). Shown are the individual ratios (±SD) of Gpr161-mCherry wild-type (12 sections, 578 cilia), Gpr161-mCherry S428D/S429D (9 sections, 584 cilia), and Gpr161-mCherry S428A/S429A (9 sections, 415 cilia). (D) Coexpression of Gpr161-mCherry and RIα-GFP in zebrafish. The graph shows the ratio of RIα, Gpr161 double-positive cilia over the total number of Gpr161-mCherry-positive cilia (mean ± SEM, Gpr161-mCherry wild-type $n = 7$ embryos, Gpr161-mCherry L465P $n = 6$ embryos). ***$P < 0.001$ using two-tailed unpaired Student's t test. (Scale bar, 5 μm.)

www.manaraa.com

showed that RIα, which is required for Hh signaling (39), localizes to the primary cilium itself (40). We have shown here that in overexpression experiments Gpr161 can recruit RIα to the primary cilium in zebrafish, consistent with the idea that Gpr161 may act directly as an RI AKAP in the primary cilium. Taken together, our results suggest that Gpr161 may play a more complex role in the regulation of PKA activity in Hh signaling.

Our findings that PKA type I R subunits bind selectively to the membrane receptor prompted us to test Gpr161 interactions with a mutated and disease-relevant RI subunit mutant. One point mutation in the RIβ D/D domain (RIβ[L50R]) affects PKA function and is associated with neurodegenerative diseases (20). This mutation is sufficient to diminish PPI with Gpr161. In addition, specific RIα mutations impair cAMP-dependent PKA activation and cause hormone resistance, as observed in distinct rare diseases (19). We speculate that such interactions of RIα*:Gpr161 complexes would desensitize compartmentalized Gpr161:PKA complexes for cAMP-activation, whereas activating mutations in RIα would reduce the recruitment of type I PKA holoenzymes to the AKAP receptor. We assume that the binary Gpr161:PKA complex acts as a compartmentalized signaling hub for integrating receptor-sensed input signals and spatiotemporal cAMP dynamics. Gpr161 is an orphan GPCR with intrinsic AKAP function. Given that GPCRs are the largest family of cell surface molecules involved in signal transmission, it would be surprising if Gpr161 is the "lone wolf" with AKAP function among more than 800 GPCRs in the human genome (46).

1. Langeberg LK, Scott JD (2015) Signalling scaffolds and local organization of cellular behaviour. *Nat Rev Mol Cell Biol* 16(4):232–244.
2. Shukla AK, Xiao K, Lefkowitz RJ (2011) Emerging paradigms of β-arrestin-dependent seven transmembrane receptor signaling. *Trends Biochem Sci* 36(9):457–469.
3. Good MC, Zalatan JG, Lim WA (2011) Scaffold proteins: Hubs for controlling the flow of cellular information. *Science* 332(6030):680–686.
4. Ritter SL, Hall RA (2009) Fine-tuning of GPCR activity by receptor-interacting proteins. *Nat Rev Mol Cell Biol* 10(12):819–830.
5. Scott JD, Dessauer CW, Taskén K (2013) Creating order from chaos: Cellular regulation by kinase anchoring. *Annu Rev Pharmacol Toxicol* 53:187–210.
6. Scott JD, Pawson T (2009) Cell signaling in space and time: Where proteins come together and when they're apart. *Science* 326(5957):1220–1224.
7. Daaka Y, Luttrell LM, Lefkowitz RJ (1997) Switching of the coupling of the beta2-adrenergic receptor to different G proteins by protein kinase A. *Nature* 390(6655):88–91.
8. Tobin AB (2008) G-protein-coupled receptor phosphorylation: Where, when and by whom. *Br J Pharmacol* 153(Suppl 1):S167–S176.
9. Rockman HA, Koch WJ, Lefkowitz RJ (2002) Seven-transmembrane-spanning receptors and heart function. *Nature* 415(6868):206–212.
10. Taylor SS, Ilouz R, Zhang P, Kornev AP (2012) Assembly of allosteric macromolecular switches: Lessons from PKA. *Nat Rev Mol Cell Biol* 13(10):646–658.
11. Wong W, Scott JD (2004) AKAP signalling complexes: Focal points in space and time. *Nat Rev Mol Cell Biol* 5(12):959–970.
12. Herberg FW, Maleszka A, Eide T, Vossebein L, Tasken K (2000) Analysis of A-kinase anchoring protein (AKAP) interaction with protein kinase A (PKA) regulatory subunits: PKA isoform specificity in AKAP binding. *J Mol Biol* 298(2):329–339.
13. Kinderman FS, et al. (2006) A dynamic mechanism for AKAP binding to RII isoforms of cAMP-dependent protein kinase. *Mol Cell* 24(3):397–408.
14. Houslay MD (2010) Underpinning compartmentalised cAMP signalling through targeted cAMP breakdown. *Trends Biochem Sci* 35(2):91–100.
15. Espiard S, Ragazzon B, Bertherat J (2014) Protein kinase A alterations in adrenocortical tumors. *Horm Metab Res* 46(12):869–875.
16. Cheung J, et al. (2015) Structural insights into mis-regulation of protein kinase A in human tumors. *Proc Natl Acad Sci USA* 112(5):1374–1379.
17. Honeyman JN, et al. (2014) Detection of a recurrent DNAJB1-PRKACA chimeric transcript in fibrolamellar hepatocellular carcinoma. *Science* 343(6174):1010–1014.
18. Zilbermint M, Stratakis CA (2015) Protein kinase A defects and cortisol-producing adrenal tumors. *Curr Opin Endocrinol Diabetes Obes* 22(3):157–162.
19. Silve C, Clauser E, Linglart A (2012) Acrodysostosis. *Horm Metab Res* 44(10):749–758.
20. Wong TH, et al.; Netherlands Brain Bank; International Parkinsonism Genetics Network (2014) PRKAR1B mutation associated with a new neurodegenerative disorder with unique pathology. *Brain* 137(Pt 5):1361–1373.
21. Stork PJ, Schmitt JM (2002) Crosstalk between cAMP and MAP kinase signaling in the regulation of cell proliferation. *Trends Cell Biol* 12(6):258–266.
22. Dumaz N, Marais R (2005) Integrating signals between cAMP and the RAS/RAF/MEK/ERK signalling pathways. Based on the anniversary prize of the Gesellschaft für Biochemie und Molekularbiologie Lecture delivered on 5 July 2003 at the Special FEBS Meeting in Brussels. *FEBS J* 272(14):3491–3504.
23. Mukhopadhyay S, et al. (2013) The ciliary G-protein-coupled receptor Gpr161 negatively regulates the Sonic hedgehog pathway via cAMP signaling. *Cell* 152(1-2):210–223.
24. Bensimon A, Heck AJ, Aebersold R (2012) Mass spectrometry-based proteomics and network biology. *Annu Rev Biochem* 81:379–405.
25. Woodsmith J, Stelzl U (2014) Studying post-translational modifications with protein interaction networks. *Curr Opin Struct Biol* 24:34–44.
26. Matteson PG, et al. (2008) The orphan G protein-coupled receptor, Gpr161, encodes the vacuolated lens locus and controls neurulation and lens development. *Proc Natl Acad Sci USA* 105(6):2088–2093.
27. Bachmann VA, et al. (2013) Reciprocal regulation of PKA and Rac signaling. *Proc Natl Acad Sci USA* 110(21):8531–8536.
28. Stefan E, et al. (2011) PKA regulatory subunits mediate synergy among conserved G-protein-coupled receptor cascades. *Nat Commun* 2:598.
29. Burgers PP, van der Heyden MA, Kok B, Heck AJ, Scholten A (2015) A systematic evaluation of protein kinase A-A-kinase anchoring protein interaction motifs. *Biochemistry* 54(1):11–21.
30. Sarma GN, et al. (2010) Structure of D-AKAP2:PKA RI complex: Insights into AKAP specificity and selectivity. *Structure* 18(2):155–166.
31. Röck R, et al. (2015) In-vivo detection of binary PKA network interactions upon activation of endogenous GPCRs. *Sci Rep* 5:11133.
32. Stefan E, et al. (2007) Quantification of dynamic protein complexes using *Renilla* luciferase fragment complementation applied to protein kinase A activities in vivo. *Proc Natl Acad Sci USA* 104(43):16916–16921.
33. Burgers PP, et al. (2016) Structure of smAKAP and its regulation by PKA-mediated phosphorylation. *FEBS J.*
34. Carr DW, et al. (1991) Interaction of the regulatory subunit (RII) of cAMP-dependent protein kinase with RII-anchoring proteins occurs through an amphipathic helix binding motif. *J Biol Chem* 266(22):14188–14192.
35. Corbit KC, et al. (2005) Vertebrate Smoothened functions at the primary cilium. *Nature* 437(7061):1018–1021.
36. Rohatgi R, Milenkovic L, Scott MP (2007) Patched1 regulates hedgehog signaling at the primary cilium. *Science* 317(5836):372–376.
37. Pal K, et al. (2016) Smoothened determines β-arrestin-mediated removal of the G protein-coupled receptor Gpr161 from the primary cilium. *J Cell Biol* 212(7):861–875.
38. Aanstad P, et al. (2009) The extracellular domain of Smoothened regulates ciliary localization and is required for high-level Hh signaling. *Curr Biol* 19(12):1034–1039.
39. Jacob LS, et al. (2011) Genome-wide RNAi screen reveals disease-associated genes that are common to Hedgehog and Wnt signaling. *Sci Signal* 4(157):ra4.
40. Mick DU, et al. (2015) Proteomics of primary cilia by proximity labeling. *Dev Cell* 35(4): 497–512.
41. Magalhaes AC, Dunn H, Ferguson SS (2012) Regulation of GPCR activity, trafficking and localization by GPCR-interacting proteins. *Br J Pharmacol* 165(6):1717–1736.
42. Malbon CC, Tao J, Wang HY (2004) AKAPs (A-kinase anchoring proteins) and molecules that compose their G-protein-coupled receptor signalling complexes. *Biochem J* 379(Pt 1):1–9.
43. Fraser ID, et al. (2000) Assembly of an A kinase-anchoring protein-beta(2)-adrenergic receptor complex facilitates receptor phosphorylation and signaling. *Curr Biol* 10(7):409–412.
44. Briscoe J, Thérond PP (2013) The mechanisms of Hedgehog signalling and its roles in development and disease. *Nat Rev Mol Cell Biol* 14(7):416–429.
45. Barzi M, Berenguer J, Menendez A, Alvarez-Rodriguez R, Pons S (2010) Sonic-hedgehog-mediated proliferation requires the localization of PKA to the cilium base. *J Cell Sci* 123(Pt 1):62–69.
46. Lagerström MC, Schiöth HB (2008) Structural diversity of G protein-coupled receptors and significance for drug discovery. *Nat Rev Drug Discov* 7(4):339–357.
47. Courcelles M, et al. (2013) Phosphoproteome dynamics reveal novel ERK1/2 MAP kinase substrates with broad spectrum of functions. *Mol Syst Biol* 9:669.
48. Beck M, et al. (2011) The quantitative proteome of a human cell line. *Mol Syst Biol* 7:549.
49. Courcelles M, Lemieux S, Voisin L, Meloche S, Thibault P (2011) ProteoConnections: A bioinformatics platform to facilitate proteome and phosphoproteome analyses. *Proteomics* 11(13):2654–2671.
50. Schwartz D, Gygi SP (2005) An iterative statistical approach to the identification of protein phosphorylation motifs from large-scale data sets. *Nat Biotechnol* 23(11): 1391–1398.
51. Kim C, Cheng CY, Saldanha SA, Taylor SS (2007) PKA-I holoenzyme structure reveals a mechanism for cAMP-dependent activation. *Cell* 130(6):1032–1043.
52. Brown SH, Wu J, Kim C, Alberto K, Taylor SS (2009) Novel isoform-specific interfaces revealed by PKA RIIbeta holoenzyme structures. *J Mol Biol* 393(5):1070–1082.
53. Schindelin J, et al. (2012) Fiji: An open-source platform for biological-image analysis. *Nat Methods* 9(7):676–682.
54. Lacroix E, Viguera AR, Serrano L (1998) Elucidating the folding problem of alpha-helices: Local motifs, long-range electrostatics, ionic-strength dependence and prediction of NMR parameters. *J Mol Biol* 284(1):173–191.

BIOCHEMISTRY

Bachmann et al.